EFCF-ID: B0909

Copper-containing fuel electrodes for solid oxide electrolysis cells

Carolin E. Frey (1), Nikolas Grünwald (1), Norbert H. Menzler (1), Olivier Guillon (1,2)
(1) Forschungszentrum Jülich GmbH, Institute of Energy and Climate Research (IEK), IEK-1: Materials Synthesis and Processing, D-52425 Jülich
(2) JARA-Energy, Jülich/Aachen
Tel.: +49-2461-619701
n.gruenwald@FZ-juelich.de

Abstract

In fuel electrodes for solid oxide electrolysis cells (SOECs) several degradation phenomena can be found after operation for prolonged duration. The agglomeration, especially the depletion of nickel in the active electrode, is the most pronounced degradation within steam electrolysis. Operating SOECs in co-electrolysis mode, coke formation in the fuel gas electrode can lead to further degradation. For nickel catalysts in methanol synthesis copper nickel alloys are known to inhibit coke formation. Therefore copper nickel alloys are interesting candidates for catalysts in SOEC fuel electrode functional layer as they might be beneficial for the suppression of nickel depletion as well.
There are many possible manufacturing routes for copper nickel alloy catalysts in solid oxide fuel or electrolysis cells. Most frequently used is the impregnation route. Disadvantages of this approach are time expanse and multiple infiltration and heating steps. In this talk alternative manufacturing routes will be pointed out. Analytical characterization will be shown.

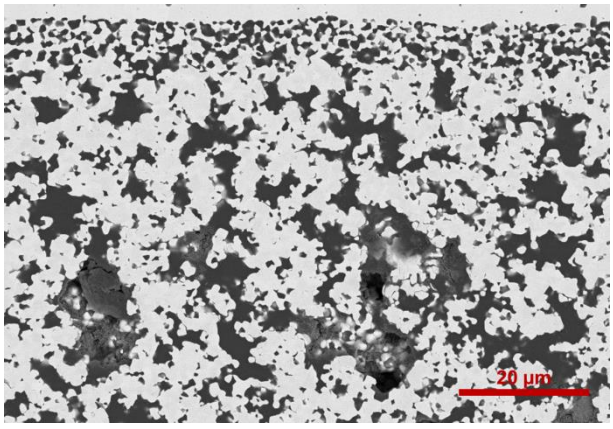

Figure 1: SEM micrograph of part of the electrolyte, the fuel electrode and the substrate of a cell operated in a stack for over 18,000 h in electrolysis mode. The high porosity of the fuel electrode is caused by nickel-depletion.

Introduction

Syngas is a valuable resource in industry that can be produced by co-electrolysis of CO_2 and H_2O within SOECs [1,2]. Disadvantageously, the presence of carbonaceous gas atmosphere induces a strong degradation of Nickel and Nickel-cermet fuel electrodes. Depending on the operation conditions, carbon species can deposit as carbon particles or carbon fibers on the Ni-surface [3,4], or can lead to metal dusting [5].
Alloying Nickel with copper can inhibit the deposition of carbon in case of a Cu-content exceeding 20 wt.% [5-7]. Due to the low melting temperature of CuO (T_m = 1326 °C) the integration into anode supported cells (ASCs) is quite complicated. The high sintering temperatures of about 1400 °C, which are necessary to obtain a dense electrolyte lead to a drop in the solubility of Cu within the Cu-Ni-O-system. Thus, CuO is partly melting within CuO-NiO mixtures by exceeding a temperature of 1090 °C [8].

1. Scientific Approach

One opportunity to bypass the problem with the low melting temperature of CuO is the integration of Cu by impregnation after the full cell is already sintered. Therefore, the cell manufacturing is performed with a porous YSZ electrode layer instead of a Ni-YSZ cermet. After the cathode sintering step Cu-Ni-O is introduced into the porous YSZ by impregnation [7,9]. This technique requires several impregnation and drying processes which increases the total cell manufacturing costs.
Vacuum slip casting is chosen in this work as a more cost-efficient manufacturing route. The idea is to provide a high amount of Cu to obtain a reasonable amount of Cu within the electrode's Ni-phase after electrolyte sintering. Therefore, two approaches were tested:

1. Slip casting of pure CuO on top of a regular Ni-YSZ fuel electrode.
2. Slip casting of a mixture of CuO and YSZ on top of a regular Ni-YSZ fuel electrode.

2. Experiments

Coarse CuO powder was milled with ethanol, polyethylenimine and ZrO_2 balls for 168 h. After a sedimentation process for 5 h and 10 min the upper 80% of the suspension were extracted and a particle size distribution of d_{10} = 0.3 µm, d_{50} = 0.45 µm and d_{90} = 1.04 µm was obtained. In case of the samples with pure CuO-coating, the suspension was diluted with ethanol to obtain a solid content of 2.76 mg*ml^{-1}. For CuO-YSZ coatings a mixture of 33 mol% 8YSZ and 67 mol% CuO was diluted in ethanol to obtain 2.45 mg*ml^{-1}.
Standard Jülich anode supported cells - consisting of a 500 µm thick, tape cast Ni-8YSZ support and a 7 µm thick, screen printed Ni-8YSZ electrode layer - were used as substrate material. The CuO and CuO-8YSZ suspensions were applied by vacuum slip casting (VSC). The coating process was performed within two steps with a pressure of 600 mbar. The second step was conducted, after the first layer has dried.
All samples were coated with a 10 µm thick, screen printed 8YSZ electrolyte to evaluate the usability of the two Cu-containing layers within SOECs. The cells were sintered for 5 h at 1400 °C to densify the electrolyte. Investigations were performed using a Zeiss Ultra55 (Carl Zeiss Microscopy GmbH, Oberkochen, Germany) scanning electron microscope (SEM).

3. Results and Discussion

Figure 2 shows a cross sectional SEM-image of a sample which was coated with pure CuO before screen printing the electrolyte and subsequent sintering for 5 h at 1400 °C in air. As expected, the CuO layer has molten into the Ni-8YSZ electrode layer, due to the low melting temperature of CuO. Broad gaps are visible between electrode and electrolyte. There are hardly any contact points between these layers. Some parts of the electrolyte are detached, which can also be observed in Figure 2.
It is assumed that the sintering of the electrolyte and the electrode have progressed too far when the CuO layer has molten completely. Thus, there is no sufficient bonding between the Ni-8YSZ electrode and the 8YSZ electrolyte.

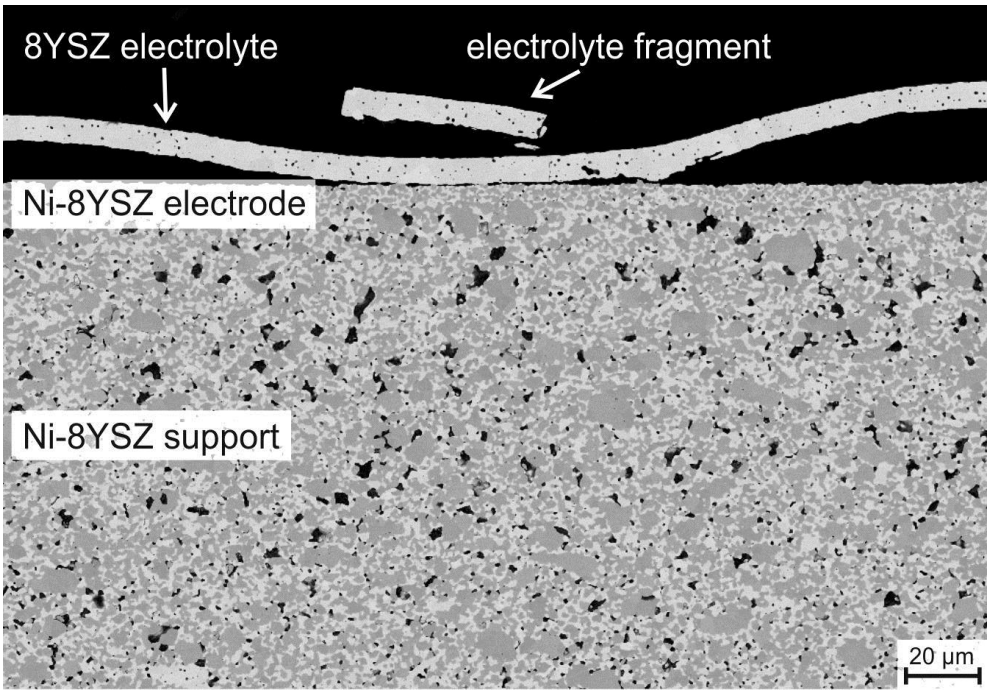

Figure 2: SEM image of a sample with pure CuO coating after 5 h sintering at 1400 °C.

EDX analysis was conducted to measure the amount of Cu within the electrode layer. A high magnification SEM image and two EDX spectra of the Ni-phase of a sample with a CuO layer after sintering are given in Figure 3. The SEM image reveals a very low porosity of the electrode, which is measured by image analysis (3.1 ± 0.5 vol.%). Measurements of the support show a porosity of 6.6 ± 0.5 vol.% in the oxidized state.
The EDX spectra at the bottom of Figure 3 indicate the presence of Cu within the Ni phase. Additional EDX point analyses, which are not shown here show that Cu can be found in large parts of the electrode and the support. A Cu concentration of 1 wt.% at the electrolyte interface and 0.5 wt.% at the other side of the functional layer can be measured by quantitative EDX analysis.

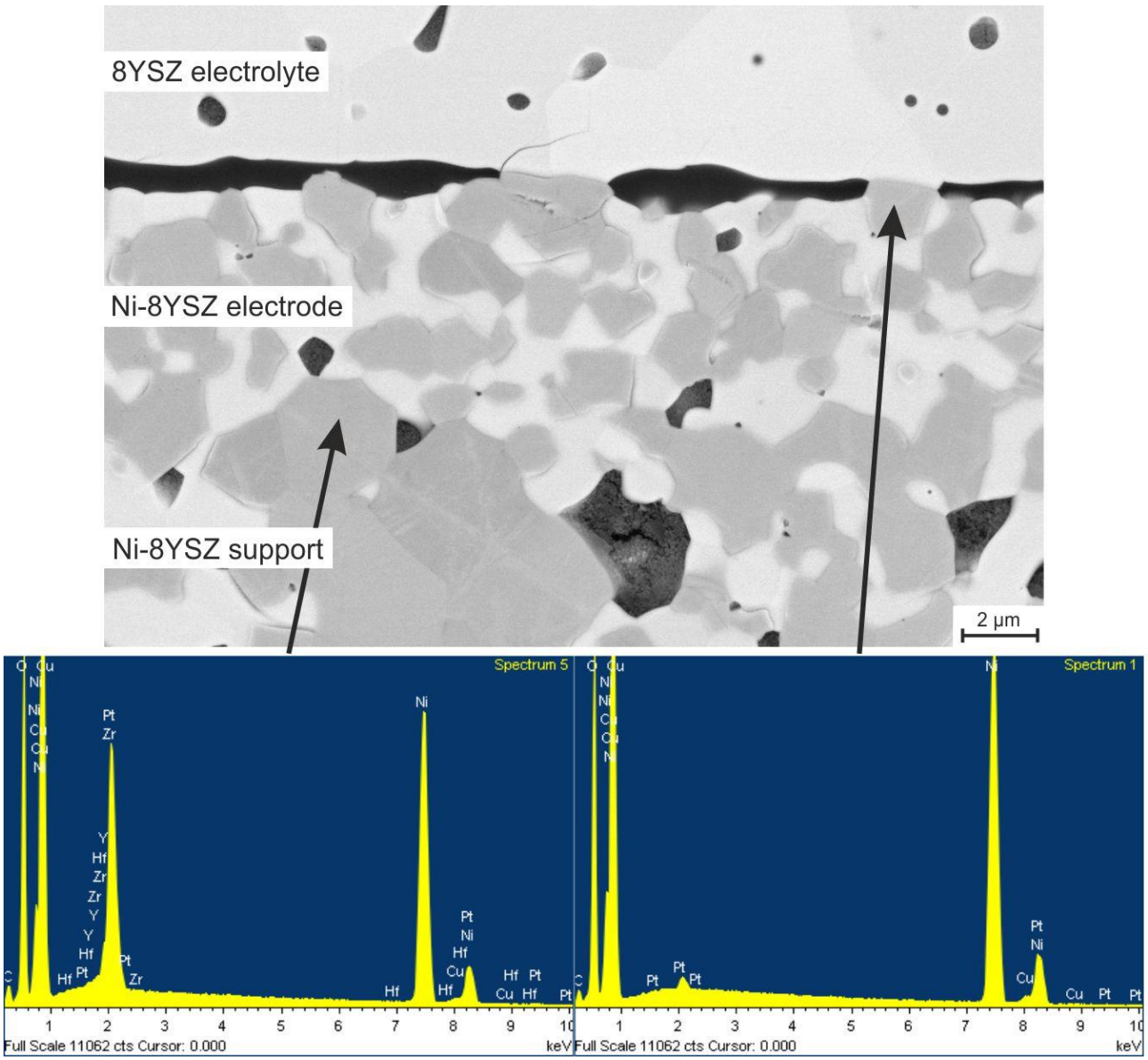

Figure 3: High magnification SEM image of a sample with pure CuO coating after sintering (top) and two EDX spectra (bottom).

To improve the adhesion between electrolyte and electrode, the CuO suspension was mixed with 8YSZ suspension as described in the experimental section. An SEM image of the sample with CuO-8YSZ coating is given in Figure 4. A 5 µm thick porous layer of 8YSZ can be observed directly underneath the dense 8YSZ electrolyte. The porous layer shows a good adhesion to both adjacent layers (the electrolyte and the electrode). EDX measurements provided in Figure 5 reveal no signals of Cu within the 8YSZ electrolyte and the porous 8YSZ layer. The CuO within the CuO-8YSZ layer has fully molten into the Ni-YSZ electrode, as observed in the first sample with a pure CuO coating. The mixture of 8YSZ serves for the necessary contact during the sintering and provides an ion conducting pathway in the sintered sample. Nevertheless, the cell performance is expected to be low due to the high porosity. Quantitative EDX analysis of the Ni-phase reveal an insufficient amount of less than 1 wt.% Cu, as observed in the Ni-phase of the sample coated with pure CuO.

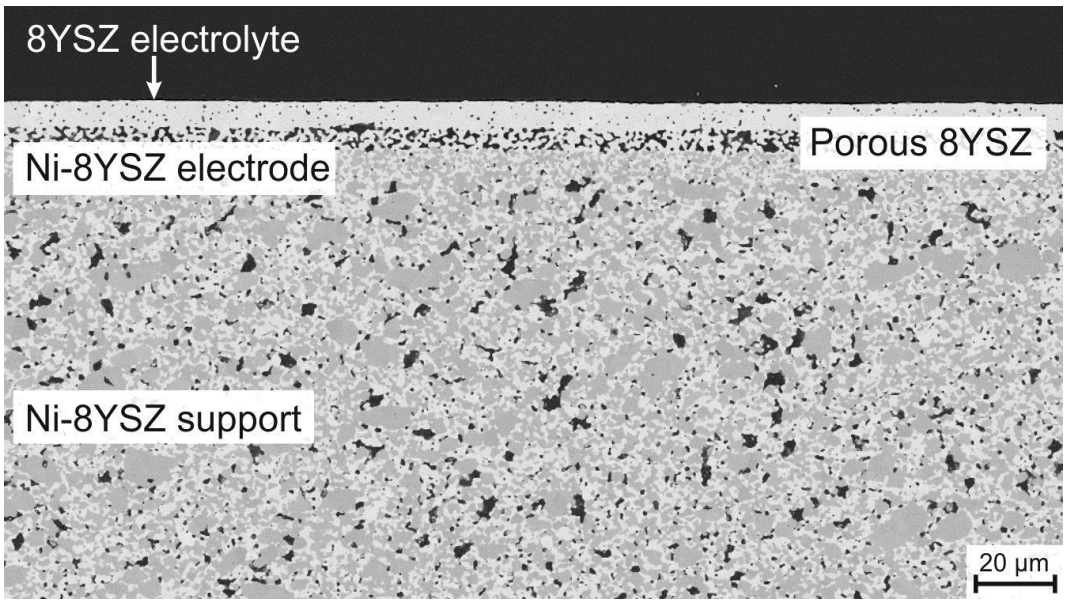

Figure 4: SEM image of a sample with CuO-8YSZ coating after 5 h sintering at 1400 °C.

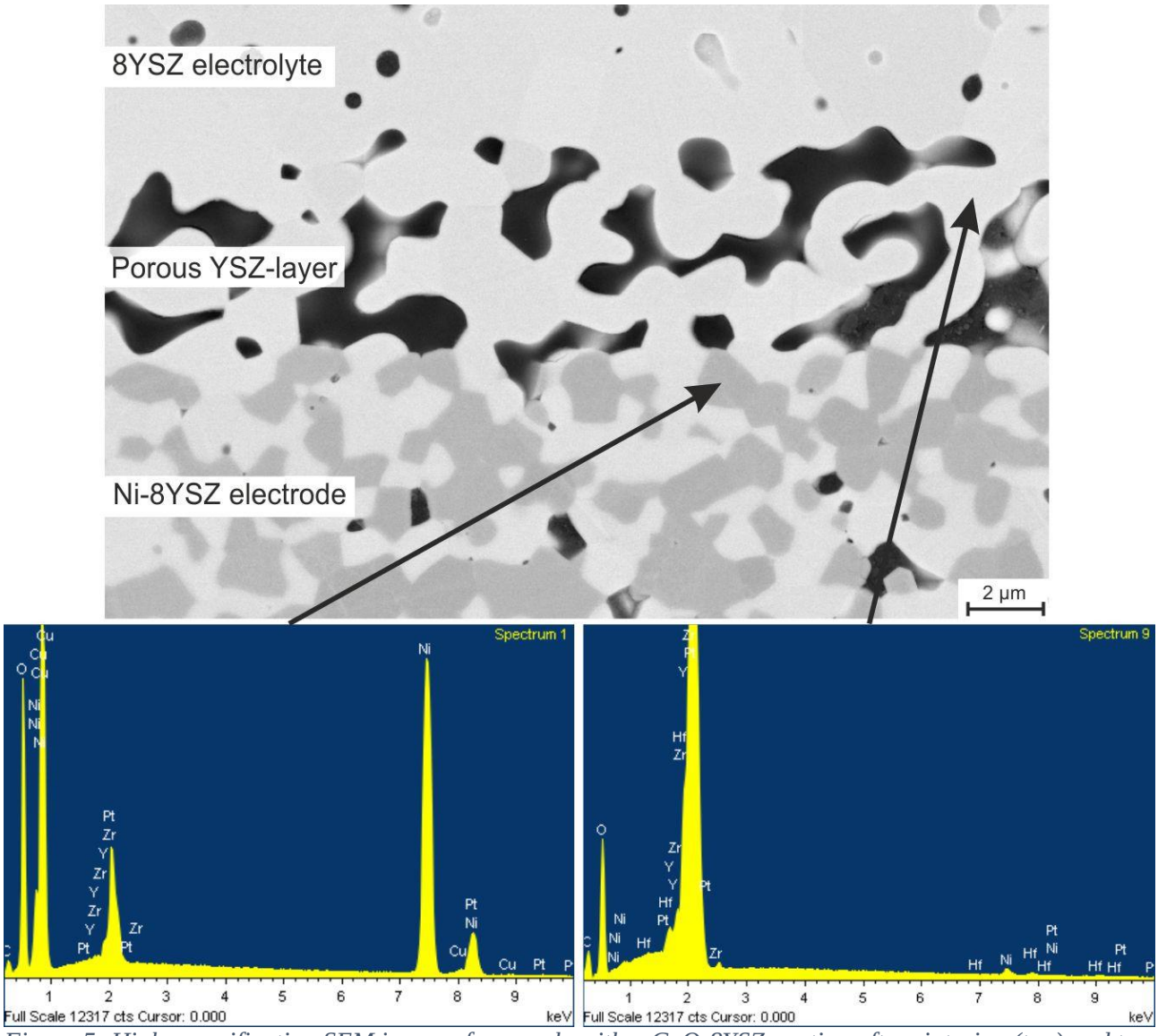

Figure 5: High magnification SEM image of a sample with a CuO-8YSZ coating after sintering (top) and two EDX spectra (bottom).

The sintering temperature of 1400 °C is too high for integrating the required amount of 20 wt.% Cu within Ni electrodes. Thus, other processing routes have to be chosen for manufacturing the electrolyte to enable a lowering of the sintering temperature.
Electrolyte supported cells with a NiO-CuO-YSZ electrode are under investigation to evaluate the electrochemical performance and the protective capability versus carbon deposition.

4. Conclusion

Alloying Ni electrodes with Cu can diminish C-deposition within SOEC co-electrolysis, if exceeding a concentration of 20 wt.%. The low melting temperature of CuO is impeding the integration in an anode supported cell due to the high sintering temperature, which is necessary to densify the electrolyte. VSC was chosen as manufacturing route to integrate Cu in the Ni-electrode in this study. Therefore two attempts were tested: 1. using pure CuO and 2. using a mixture of CuO and 8YSZ. SEM and EDX analyses of the samples coated with pure CuO showed insufficient adhesion of the electrolyte to the electrode layer. The adhesion could be improved by adding 8YSZ to the CuO suspension used for VSG. Despite the sufficient adhesion of electrode and electrolyte, the coating is not fulfilling its task, as the Cu content is too low. One opportunity to prevent the melting of CuO is to change the manufacturing route of the electrolyte. Dense electrolyte layers can be obtained by magnetron sputtering or physical vapor deposition making an adjacent sintering unnecessary [10]. Impedance spectroscopic measurements of cells with Ni-Cu fuel electrodes are ongoing to evaluate the electrochemical performance and degradation tolerance against carbon deposition and nickel migration.

References

[1] Y. Zheng, J. Wang, B. Yu, W. Zhang, J. Chen, J. Qiao, J. Zhang, Chemical Society reviews 46 (2017) 1427–1463.
[2] J.P. Stempien, Q. Liu, M. Ni, Q. Sun, S.H. Chan, Electrochimica Acta 147 (2014) 490–497.
[3] Y. Tao, S.D. Ebbesen, M.B. Mogensen, Journal of Power Sources 328 (2016) 452–462.
[4] N.Q. Minh, J American Ceramic Society 76 (1993) 563–588.
[5] Y. Nishiyama, N. Otsuka, MSF 522-523 (2006) 581–588.
[6] Y. Nishiyama, K. Moriguchi, N. Otsuka, T. Kudo, Materials and Corrosion 56 (2005) 806–813.
[7] H. Kim, C. Lu, W.L. Worrell, J.M. Vohs, R.J. Gorte, J. Electrochem. Soc. 149 (2002) A247.
[8] H. Eric, M. Timuçin, MTB 10 (1979) 561–563.
[9] S.-I. Lee, J.M. Vohs, R.J. Gorte, J. Electrochem. Soc. 151 (2004) A1319.
[10] R. Nédélec, S. Uhlenbruck, D. Sebold, V. Haanappel, H.-P. Buchkremer, D. Stöver, Journal of Power Sources 205 (2012) 157–163.